Mon. Not. R. astr. Soc. (1970) **148,** 173–191.

A NUMERICAL MODEL OF HYDROMAGNETIC TURBULENCE

D. L. Moss

(Received 1969 December 22)

SUMMARY

A kinematic numerical model of two-dimensional hydromagnetic turbulence is developed to investigate the amplification of an externally maintained seed magnetic field under the action of fluid motions of varying magnetic Reynolds number. The dependence of the degree of amplification of the mean square field on the Reynolds number is found to agree approximately with the order of magnitude estimate given. In astrophysical applications an initially weak magnetic field may often be amplified to equipartition with the velocity field. The model is applied to the problem of the expulsion of flux from a turbulent region in a conducting fluid, and it is suggested that some flux may always remain in such a region. The turbulent dynamo problem is briefly discussed.

1. INTRODUCTION

Magnetic fields and turbulent motions are connected in many problems of astrophysical interest; for example in the convection zones of lower main sequence and pre-main sequence stars, star formation, and the motions of interstellar gas clouds. The problem of the interaction of a compressible velocity field and a magnetic field is non-linear and difficult to treat self consistently even for non-turbulent motions. When the velocity field is turbulent only a statistical treatment can be attempted and for hydromagnetic turbulence this proves difficult. There has been dispute, for example, as to whether a large-scale field which is maintained by an external e.m.f. will be amplified indefinitely in the absence of a back reaction of the Lorentz forces on the fluid, or whether the growth will in any case be limited by Ohmic dissipation. (See e.g. Biermann & Schluter 1951; Saffmann 1963, 1964; Vainshtein 1969.)

Weiss (1966) investigated the effects of an inexorable, non-divergent velocity field simulating convective cells on a seed magnetic field by following numerically the time evolution of the system. True turbulent motion is rather different in character—for example there are now no favoured ' dead zones ' into which the field lines can be convected, concentrated into ropes, and left in a steady state with the effects of resistive decay being balanced by the convective effects. No true steady state is to be expected, and so it is not now obvious that ropes of flux will be formed as they are in a model with simple fixed cells.

It must be stressed that what will be considered in most of this paper is a model of an ' amplification process ' acting on a magnetic field which is assumed to be so weak that it does not act back on the fluid motions, and not a ' turbulent dynamo '. A turbulent dynamo must maintain the mean square field after the e.m.f. maintaining the seed field has been turned off, but in the model considered the seed field is always present as a consequence of the boundary conditions.

A simple numerical model of the action of two dimensional turbulent motions on a weak magnetic field is set up, and the amplification of the root mean square (r.m.s.) field examined. There are two basic parameters in the problem, the magnetic Reynolds number, R_m, and a quantity which is essentially the ratio of the scale of the turbulence to the initial field scale. Order of magnitude arguments are given to explain the results. These show that $\langle\!\langle B^2\rangle\!\rangle_t/B_0^2 \propto R_m^{\alpha}$ where $\alpha \sim 0{\cdot}70$, and that the dependence of $\langle\!\langle B^2\rangle\!\rangle_t/B_0^2$ on the ratio of the scale of the turbulence to the field scale is small. In this work the simple parenthesis, $\langle\ \rangle$, are used to denote a space average, and the subscripted parentheses, $\langle\ \rangle_t$, for a time average.

The numerical model is adapted to treat the situation in which a turbulent zone is surrounded by a static, conducting region of fluid. It is found that all flux is not expelled from the turbulent zone, but what remains is largely concentrated into ropes. The r.m.s. field in the turbulent zone is still greater than the seed field. The electromagnetic units used throughout are rationalized gaussian units with the velocity of light taken as unity. The energy density of the magnetic field is thus $B^2/2$.

2. THE PROBLEM ATTEMPTED

The treatment is two dimensional, and, as implied above, purely kinematic, the fluid velocities being prescribed. This means that in any application of these results we must have $B^2/2 \ll 1/2\rho v^2$. For a medium with constant conductivity σ Maxwell's equations become in the ' M.H.D. approximation '.

$$\nabla \times \mathbf{H} = \sigma(\mathbf{E} + \mathbf{v} \times \mathbf{B}),$$

which gives

$$\frac{\partial B}{\partial t} = \nabla \times (\mathbf{v} \times \mathbf{B}) - \eta \nabla \times (\nabla \times B) \qquad (2.1)$$

where $\eta = 1/\mu\sigma$ is the c.g.s. resistivity.

For the two-dimensional case there is only one non-zero component of the vector potential **A**, say the z-component. So equation (2.1) becomes

$$\frac{\partial A}{\partial t} = -\mathbf{v}.\nabla A + \eta \nabla^2 A \qquad (2.2)$$

where **v** is the fluid velocity (in the (x, y) plane). The magnetic field **B** is also in the (x, y) plane.

The turbulent velocity field was simulated by considering the separation of any two points moving with the fluid to be governed by a random walk process. The magnitude of the velocity field was taken as everywhere constant, $= v_t$ say. It would have been possible to have set up the model with a variable turbulent velocity, but it was felt that taking a constant value of v_t would still give results of general interest. The velocities were generated by superposing on the two-dimensional mesh used for integration a 5×5 ' supergrid '. See Fig. 1. At any one time a random number between 0 and 1 was assigned to each of these ' supergrid ' points. This random number determined the direction of the velocity vector uniformly in the range 0 to 2π at each of the supergrid points. At intermediate points the direction of the velocity vector was obtained by linear interpolation among the values at the supergrid points. At time intervals ΔT fresh random numbers were generated and new directions for the velocity vectors determined. This velocity field was thus uncorrelated with the previous one, and so the procedure defined a stochastic

process. At times between reassignments of the velocity vectors, the direction of the velocity vector at any given point on the full grid was determined by linear interpolation in time between the values of the random numbers at that point at the neighbouring times of reassignment.

The random numbers used were pseudo-random in the sense that any sequence, although satisfying the usual criteria for randomness, could be regenerated, and so the velocity field used for the complete computation could be used again when

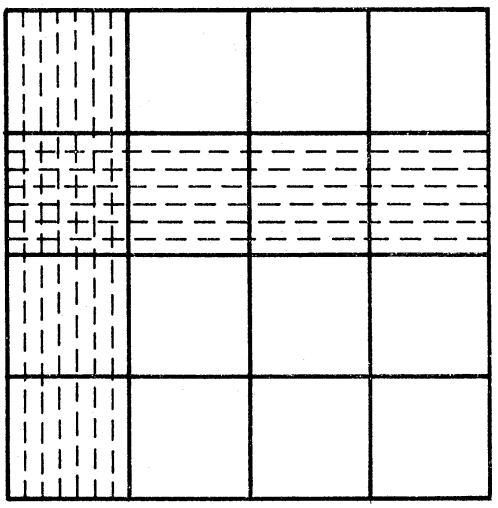

FIG. 1. *The supergrid (solid lines) and part of the grid (dashed) used for the integrations.*

necessary at a subsequent run of the program. The number of supergrid points was chosen as 25 as a compromise, arrived at by trial and error, between the desire to have as many points as possible to make the velocities over the grid as uncorrelated as possible, and the need for numerical accuracy without having too many points on the full integration grid.

The velocity fields thus generated are not incompressible at any given time, but the time average of $\nabla.\mathbf{v}$ will be zero. So the velocity fields used are, in this sense, statistically steady.

The equation (2.2) can be reduced to dimensionless form by putting

$$\begin{aligned} x' &= x/\lambda \\ y' &= y/\lambda \\ \mathbf{v}' &= \mathbf{v}/v_t \\ \tau &= tv_t/\lambda \end{aligned} \tag{2.3}$$

where λ is the distance between the supergrid points. Then

$$\frac{\partial A}{\partial \tau} = -\mathbf{v}'.\nabla_{x'}A + R_m^{-1}\nabla_{x'}{}^2A, \tag{2.4}$$

defining $R_m = v_t\lambda/\eta$, the magnetic Reynolds number. With a 5×5 supergrid the area of integration is $|x'|, |y'| \leq 2$. The other free parameter in the problem is the time interval, ΔT, between successive re-randomizations of the velocity field, which in dimensionless form becomes $\Delta T' = \Delta T v_t/\lambda$. (In some applications, e.g. to turbulent gas clouds in the Galaxy, it might be expected that $\Delta T' \sim 1$, but it is

possible that in, say, stellar convection zones, $\Delta T' < 1$). ΔT is a time scale for the turbulence and λ defines a basic length scale. The physical interpretation of these dimensionless parameters is discussed further in Section 5. The velocity field at any time could be Fourier analysed into components which would correspond instantaneously to circulation cells of various sizes with typical dimension λ.

The boundary condition taken in most cases was to have perfectly conducting walls at $y = \pm a/2$, where a is the linear dimension of the (square) grid.

Then

$$\frac{\partial \mathbf{B}}{\partial t} = -\nabla \times \mathbf{E}$$

and

$$\mathbf{B} = \nabla \times \mathbf{A}'$$

imply

$$\frac{\partial A'}{\partial t} = -E + \nabla \psi$$

where ψ is an arbitrary scalar.

Define

$$\mathbf{A} = \mathbf{A}' + \int^t \nabla \psi(\tau)\, d\tau$$

and then

$$\frac{\partial \mathbf{A}}{\partial t} = -\mathbf{E}.$$

At the boundary with the perfect conductor, $E_z = 0$.

So

$$\frac{\partial A}{\partial t} = 0 \quad \text{on} \quad y = \pm a/2, \tag{2.5}$$

is the required boundary condition.

The boundary condition in x was that the configuration be periodic in x with period a. To make the velocity field consistent the same random numbers were assigned to the supergrid points with $x = -a/2$ as to those with $x = a/2$ and the same y value. Over the two or three (according to the size of the integration grid) grid points next to $|y| = a/2$ the magnitudes of the velocities were made to tend to zero at $|y| = a/2$. Initially the magnetic field was taken to be uniform in the y direction, and to be such that $\langle B_0^2 \rangle = 0{\cdot}0625$ in arbitrary units.

Equation (2.4) was integrated using difference representations for the terms on the right-hand side and a Runge-Kutta method to perform the time integration. The convective term was represented to fourth order accuracy in the space variables, and the second derivative to second order. As the Reynolds number was large both terms on the right-hand side were thus represented to comparable accuracy. A fourth order Runge-Kutta method was used. When the Reynolds number is large this can be shown to be a reasonably efficient procedure, and it has the advantage of being simple to program. The program was tested by integrating this equation for the (dimensionless) velocity field given by the stream function

$$\psi = 0{\cdot}331(1 - 4x'^2)^2(1 - 4y'^2)^2, \tag{2.6}$$

over the region $|x'| \leq 1/2$, $|y'| \leq 1/2$, which describes a single cell, (and no random velocity components), for a range of Reynolds numbers; and comparing the dependence of $\langle B^2 \rangle / B_0^2$, the mean value of B^2/B_0^2 over the grid, on R_m with that

obtained by Weiss (1966). The least squares slope of $\log(\langle B^2\rangle/B_0^2)$ in the final steady state against $\log R_m$ was found to be 0·41, compared with Weiss' value of 0·42 for the stream function

$$\psi = -\frac{1}{\pi}(1-4y^2)^4 \cos \pi x.$$

3. ORDER OF MAGNITUDE ESTIMATES

Before describing the numerical results obtained it is of interest to look at some order of magnitude arguments which might apply to the problem being considered.

Consider a region between two perfectly conducting walls with an initially uniform field perpendicular to these walls. (See Fig. 4a.) Suppose the motions of the fluid particles are describable by a random walk process, and that the time between redefinitions of direction of motion of such particles is ΔT.

In time T there are $T/\Delta T$ steps, and therefore a particle suffers a mean net displacement

$$v_t \Delta T \left(\frac{T}{\Delta T}\right)^{1/2} = v_t (T\Delta T)^{1/2},$$

where v_t is the magnitude of the turbulent velocity. So the effective velocity of the particle as measured over a time interval $T \gg \Delta T$ has magnitude

$$v_{\text{eff}} = \frac{v_t (T\Delta T)^{1/2}}{T} = v_t \left(\frac{\Delta T}{T}\right)^{1/2}. \tag{3.1}$$

Consider the effects of the random motions at any time to be effectively that of a set of eddies each with properties similar to the circulation cells investigated by Weiss. The magnetic field lines obtained as the result of the computations (e.g. Figs 11, 12 and 13) illustrate the motivation for looking at the random motions in this way. From the results of Weiss the dimensionless time, $\tau_{\max}$, for the value of $\langle B^2\rangle$ to reach a maximum can be found as a function of the Reynolds number. (Typically the time dependence of $\langle B^2\rangle$ on t for a circulation cell is as shown in Fig. 2.) If $\log \tau_{\max}$ is plotted against $\log R_{mc}$, where R_{mc} is the magnetic Reynolds

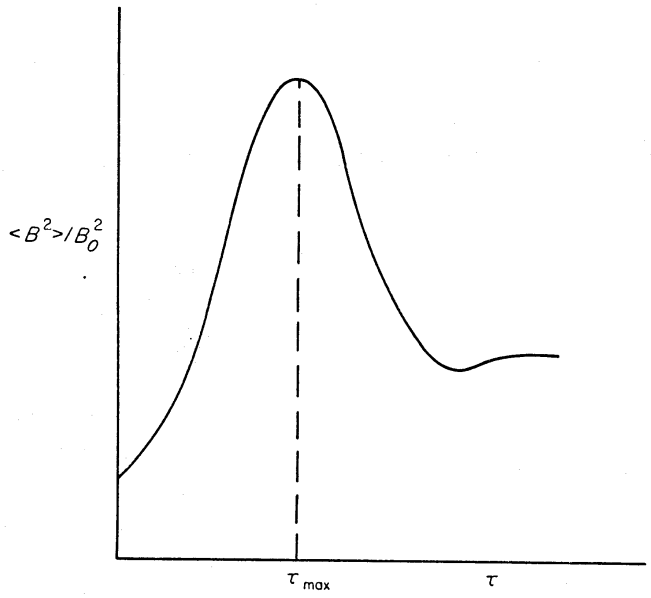

FIG. 2. *Typical dependence of* $\langle B^2\rangle$ *on* τ *for a circulation cell.*

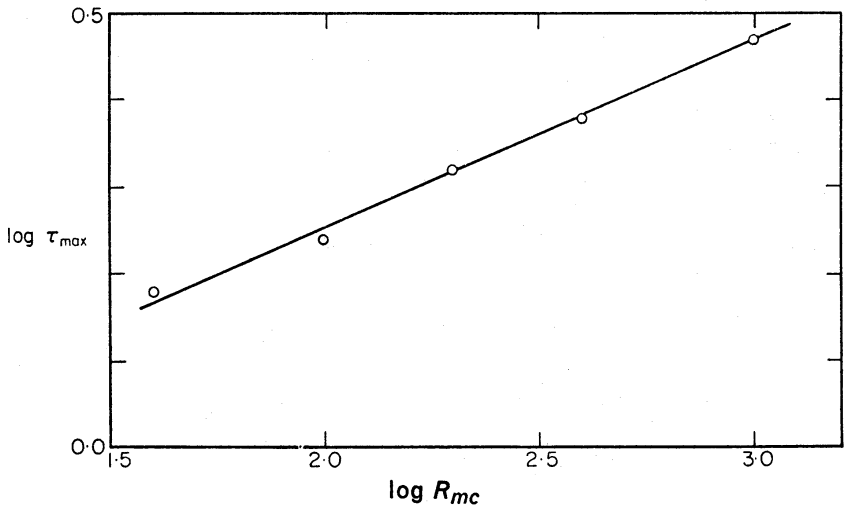

FIG. 3. *Log τ_{max} against log R_{mc} for Weiss circulation cells.*

number for the cellular motion, $= UL/\eta$, a straight line results of slope $\simeq 0{\cdot}21$, see Fig. 3.

So

$$T_{\max} \propto \frac{L}{U} R_{mc}{}^{\alpha}, \tag{3.2}$$

where $\alpha \simeq 0{\cdot}21$ from Weiss' results and 0·25 from integrations with the stream function (2.6). $T_{\max}$ is the time corresponding to $\tau_{\max}$, L is the linear dimension of the cell and U a typical cell velocity.

The mean square field will grow until the resistive decay time equals a typical amplification time. But substituting v_{eff} for U in relation (3.2) (and putting $R_{mc} = UL/\eta$), gives the estimate

$$T_{\max}\alpha \left(\frac{v_t \left(\frac{\Delta T}{T_{\max}}\right)^{1/2} L}{\eta}\right)^{\alpha} \frac{L}{v_t \left(\frac{\Delta T}{T_{\max}}\right)^{1/2}} = \left(\frac{v_t L}{\eta}\right)^{\alpha} \left(\frac{\Delta T}{T_{\max}}\right)^{(\alpha-1)/2} \left(\frac{L}{v_t}\right), \tag{3.3}$$

so

$$T_{\max} \propto \left(R_m{}^{\alpha} \frac{L}{v_t}\right)^{2/(1+\alpha)} \frac{1}{\Delta T^{(1-\alpha)/(1+\alpha)}}, \tag{3.4}$$

where R_m is the Reynolds number as defined for the turbulent motion in terms of its typical wavelength L.

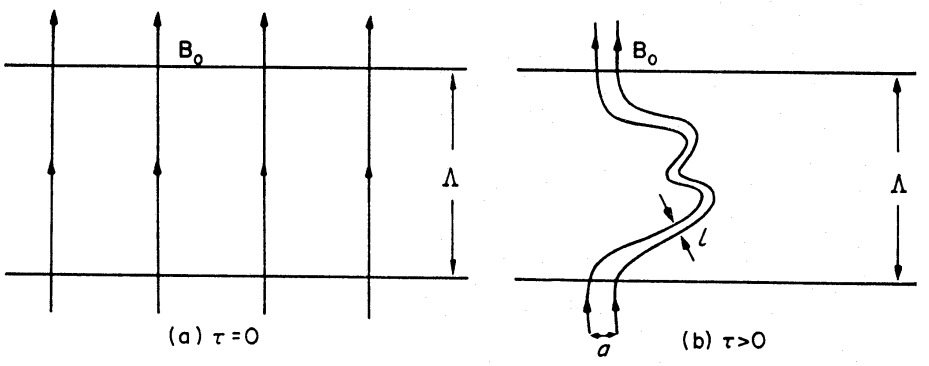

FIG. 4. *See text.*

Now as the turbulent motion distorts the field it reduces its length scale. In particular look at a tube of flux such as AA', Fig. 4. Suppose initially it has extent a in the dimension perpendicular to the field, and its length subsequently increases from Λ to $\xi\Lambda$ and $a \to l$ typically in the fluid.

Then, since the magnetic Reynolds number is large and the fluid is, in the mean, incompressible, conservation of flux implies $a\Lambda \sim \xi\Lambda l$, until resistive effects become important,

i.e.

$$l \sim a/\xi.$$

The resistive decay time is $l^2/\eta \sim a^2/\xi^2\eta$, and $B^2 \sim B_o{}^2\xi^2$.

The mean square field will be amplified until

$$T_{\max} \sim \frac{a^2}{\xi^2\eta} \sim \frac{L^2}{\xi^2\eta} \tag{3·5}$$

if the original thickness of the rope is taken equal to the typical scale L. This gives

$$\xi^2 \gtrsim (R_m \Delta T')^{(1-\alpha)/(1+\alpha)}. \tag{3·6}$$

For $\alpha = 0{\cdot}21$ this becomes

$$\langle\langle B^2 \rangle\rangle_t / B_0{}^2 \sim \xi^2 \sim (R_m \Delta T')^{0{\cdot}65}, \tag{3·7}$$

and for $\alpha = 0{\cdot}25$

$$(1-\alpha)/(1+\alpha) \simeq 0{\cdot}60.$$

These values 0·60, 0·65 are not, of course, to be taken as exact predictions for the turbulent problem, but rather as estimates of the possible range of values of the amplification factor.

These predictions are to be compared with the result $\langle\langle B^2 \rangle\rangle_t / B_0{}^2 \gtrsim R_m$ if the reasoning of Parker (1963) is followed exactly, but for two-dimensional motions rather than the three-dimensional motions he considered. The difference lies in treating the turbulent motions, at any one time, as being capable of being analysed into cells, with the relevant velocity being given by (3.1), and this velocity essentially determining the amplification time given by the estimate (3.2) for the field. Parker used a/v_t as an estimate of the amplification time.

4. NUMERICAL RESULTS

(a) For the first sequence of computations $\Delta T'$, the dimensionless time interval between re-randomizations of the velocity field, was kept fixed and R_m varied. $\Delta T'$ was given the value 0·15 which was equal to the value of the time step, $\Delta\tau$, and integrations were performed for Reynolds numbers of 25, 50, 80, 200 and 400. The same sequence of random numbers was used in each case, so the velocity fields as a function of time were the same.

Results are shown in Fig. 5. (In this and subsequent figures it should be noted that values of $\langle B^2 \rangle$ are plotted at every fifth time-step $\Delta\tau$ (usually), and so the straight lines joining the plotted points are only to be regarded as schematic.) The first two computations were done on a 29×29 grid, and the last three on a 41×41 grid. These grid sizes were shown to be adequate by comparing the results of integrations performed on grids of varying size. It appears from these results that a statistically steady state is set up in each case. For $R_m = 25$ and 50 this occurs quite

quickly, but for cases with larger Reynolds number it is necessary to continue the computations much longer. (The computations for $R_m = 200$ and 400 were not continued for as long as the $R_m = 80$ case, but it seems from the similarity in form of the changes in the mean field at different Reynolds number that in all cases a statistically steady state has been reached.) A little arbitrarily, $\tau = 7{\cdot}5$ was taken to correspond to the setting up of the steady state. Time averages of $\langle B^2 \rangle$ were calculated for $7{\cdot}5 \leq \tau \leq 30{\cdot}5$ (except for the $R_m = 50$ case where the average was taken

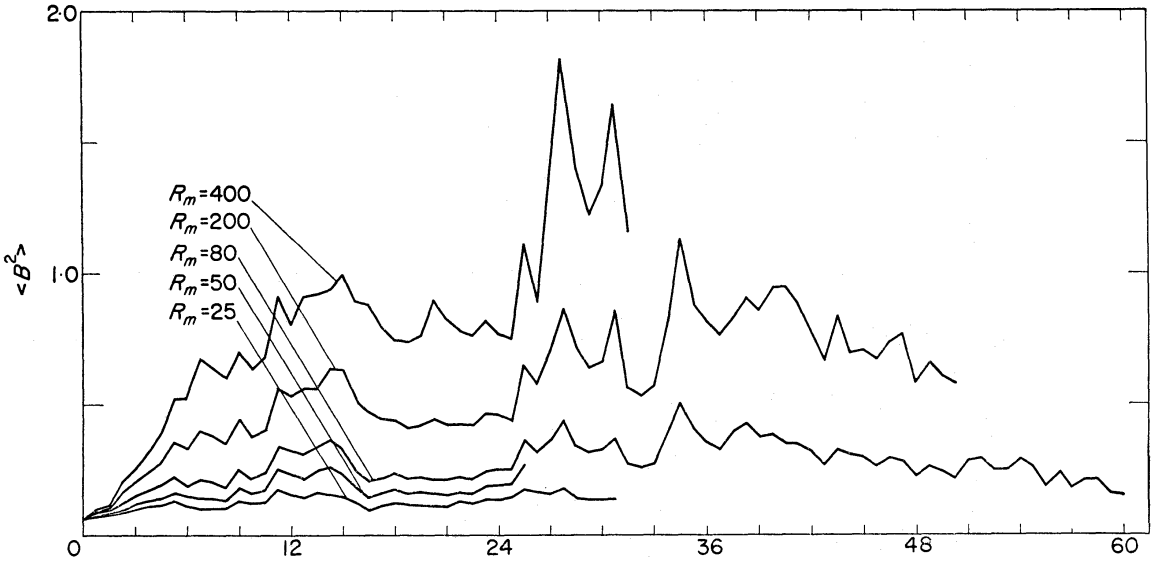

FIG. 5. *The run of $\langle B^2 \rangle$ with τ for $\Delta T' = 0{\cdot}15$. The curves are labelled with their magnetic Reynolds numbers. $B_0^2 = 0{\cdot}0625$ in arbitrary units.*

over $7{\cdot}5 \leq \tau \leq 25{\cdot}5$). For the $R_m = 80$ case the time average was also computed over the range $7{\cdot}5 \leq \tau \leq 60$—this only changed $\langle\langle B^2 \rangle\rangle_t$ from 0·276 to 0·288.

Log $\langle\langle B^2/B_0^2 \rangle\rangle_t$ against log R_m is plotted in Fig. 6. The straight line is the least squares fit, which has slope 0·70, i.e. we have

$$\langle\langle B^2 \rangle\rangle_t / B_0^2 \propto R_m^{0{\cdot}70}. \tag{4.1}$$

Time averages of the 13th largest value of B^2 on the 29×29 and the 26th largest over the 41×41 grid were also calculated for each case. As the grids have respectively 841 and 1681 points these samples are equivalent. A least squares fit gives

$$\langle B_{\max}^2 \rangle_t \propto R_m^{1{\cdot}25} \tag{4.2}$$

although the scatter is larger—see Fig. 7. (There is no significance in the choice of the 13th and 26th largest values—this is a consequence of the form of the output specified in the program.)

(b) Calculations were performed for a second sequence, on a 29×29 grid, keeping R_m fixed at 50 and varying $\Delta T'$. Values of $\Delta T' = 0{\cdot}30$, 0·60 and 0·90 were taken (in addition to the $\Delta T' = 0{\cdot}15$ calculation described above). The results of these computations are shown in Fig. 8. One of the effects of increasing $\Delta T'$ is to increase the time scale of the oscillations of the mean square field, and to increase the relative height of the peaks. This can be clearly seen by comparing the $\Delta T' = 0{\cdot}15$ and $\Delta T' = 0{\cdot}30$ cases in Fig. 8. Minor peaks at $\tau \sim 5{\cdot}25$ and 9·0 on the $\Delta T' = 0{\cdot}15$ curve are magnified into major peaks at $\tau \sim 10{\cdot}5$ and 18·0 on the $\Delta T' = 0{\cdot}30$ curve, and the peak at $\tau \sim 11{\cdot}5$ appears at $\tau \sim 22{\cdot}5$. Again $\langle\langle B^2 \rangle\rangle t$ was calculated and

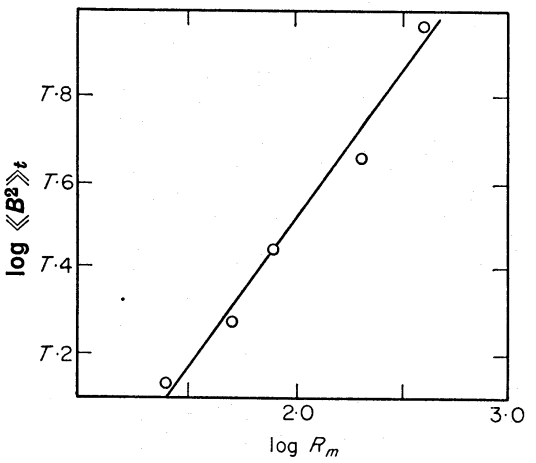

FIG. 6. *Log* $\langle\langle B^2\rangle\rangle_t$ *against log* R_m *for* $\Delta T' = 0{\cdot}15$.

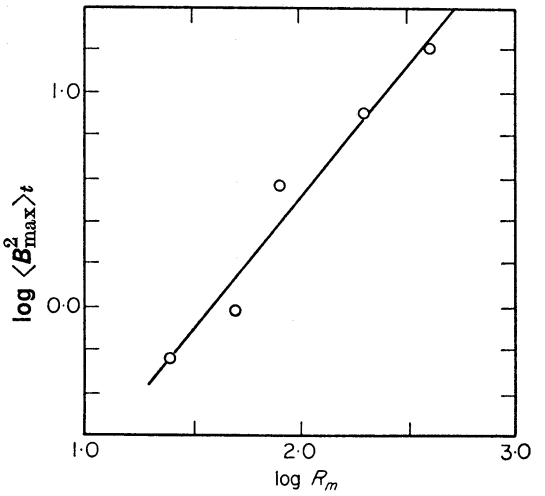

FIG. 7. *Log* $\langle B^2_{\max}\rangle_t$ *against* R_m *for* $\Delta T' = 0{\cdot}15$.

log $\langle\langle B^2\rangle\rangle_t$ against log $\Delta T'$ is shown in Fig. 9. The least squares straight line is shown and has slope 0·73, i.e.

$$\langle\langle B^2\rangle\rangle_t / B_0^2 \Delta T'^{0} \propto \cdot^{73} \qquad (4{\cdot}3)$$

(c) These slopes of 0·70 and 0·73 are to be compared with the order of magnitude estimates given above by equations (3.7). To be noted in all cases are the large oscillations, which are of statistical origin, in the r.m.s. field. Their characteristic period is much greater than $\Delta T'$.

(d) The results described above were all obtained using the same sequence of random numbers, that is the same turbulent velocity field. Because of the large number of steps of the random walk process involved in each computation, $(20 \times \tau/\Delta T')$, the averages computed should be independent of the particular set of random numbers used and the same dependence of $\langle\langle B^2\rangle\rangle_t$ on R_m and $\Delta T'$ might

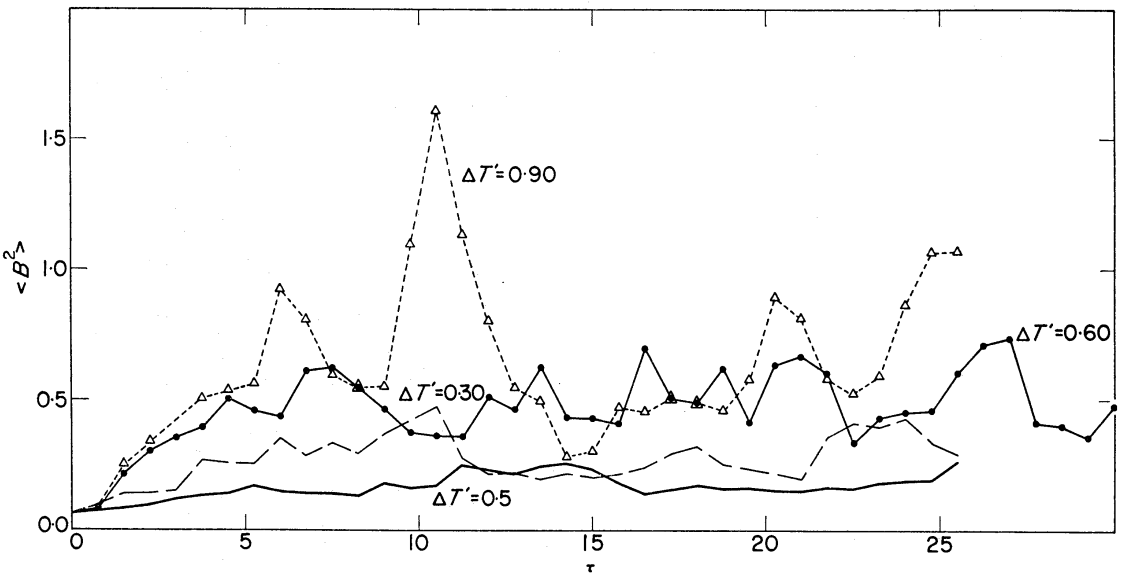

FIG. 8. *The run of* $\langle B^2\rangle$ *with* τ *for* $R_m = 50$. *The curves are labelled with the appropriate values of* $\Delta T'$.

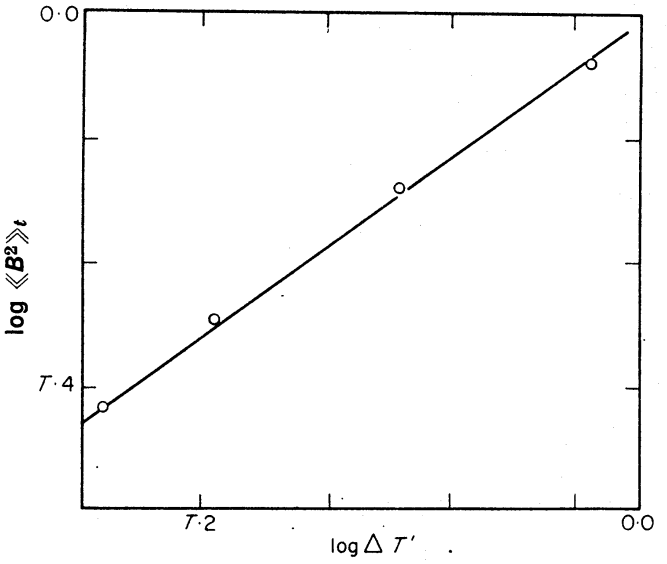

FIG. 9. *Log* $\langle\langle B^2\rangle\rangle_t$ *against log* $\Delta T'$ *for* $R_m = 50$.

be expected for each sequence. To do the problem thoroughly a number of computations should be performed at each Reynolds number with differing sequences of random numbers, and the average properties calculated at each Reynolds number. Using the same turbulent velocity fields, however, enables an easier comparison to be made of the effects of changing the parameters. To demonstrate the validity of this procedure a short run was carried out on a 29×29 grid with $R_m = 50$ and $\Delta T' = 0{\cdot}15$ and a different sequence of random numbers. This is compared with the previous $R_m = 50$, $\Delta T' = 0{\cdot}15$ computation in Fig. 10.

(e) A program was written which drew field lines for a limited number of configurations of the field for each run of the program. Typical configurations of the field for some of the computations described above are shown in Figs 11, 12 and 13. The formation of disconnected loops can be observed, and also local regions of high magnetic field. Whether a given loop has actually become disconnected is not always clear, and it is possible that some of the long loops of the field lines should really be shown as forming separate disconnected loops, and vice versa.

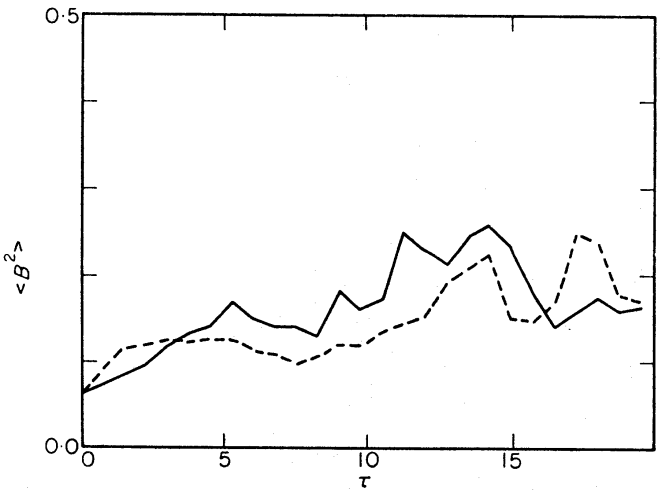

FIG. 10. *The result of choosing a different sequence of random numbers.* $R_m = 50$, $\Delta T' = 0{\cdot}15$.

5. PHYSICAL INTERPRETATION OF PARAMETERS

So far the results have been presented as a function of the two-dimensionless parameters R_m and $\Delta T'$. In applications to physical problems it is usual to work with the Reynolds number of the turbulence, say $R_m' = v_t L/\eta$, where L is now the mean free path of a turbulent element. In terms of the above parameters

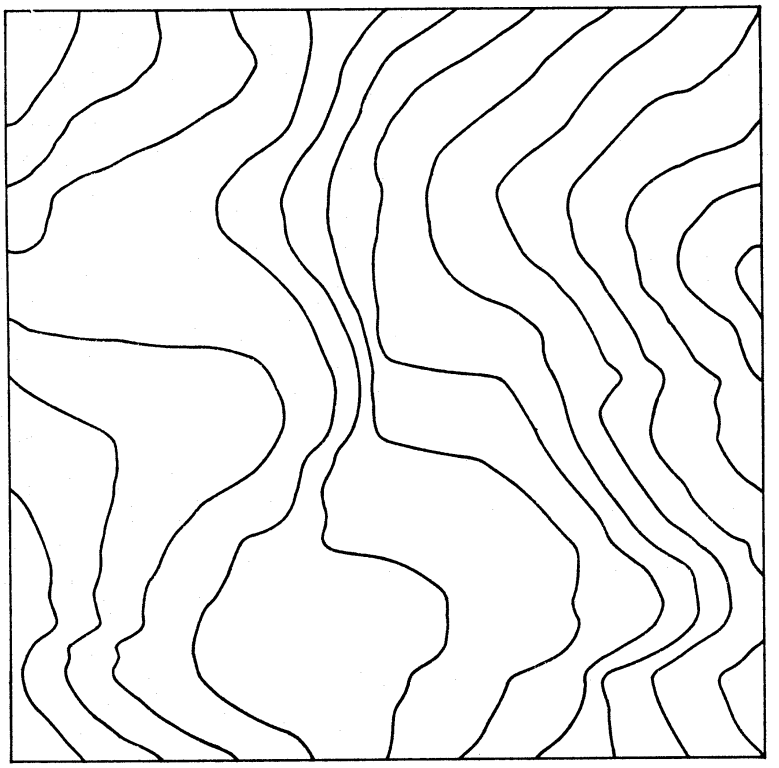

FIG. 11. *Field lines for* $R_m = 25$ *at* $\tau = 30{\cdot}75$. $\langle B^2 \rangle = 0{\cdot}14$.

$R_m' = \Delta T' R_m$. Also $L = v_t \Delta T$, and if λ is the ' distance between random sources ', i.e. a length scale for the large-scale field, then $L/\lambda = \Delta T'$ is the ratio of the scale of the magnetic field. The sequence of computations with $\Delta T'$ constant thus have $R_m' = 3{\cdot}75$, $7{\cdot}5$, 12, 30 and 60, and the result (4.1) of Section 4(a) becomes $\langle\langle B^2 \rangle\rangle_t / B_0^2 \propto R_m'^{0{\cdot}70}$ for fixed $\Delta T'$.

The result (4.3) of Section 4(b) for fixed R_m can then be interpreted as

$$\frac{\langle\langle B^2 \rangle\rangle_t}{B_0^2} \propto \left(\frac{L}{\lambda}\right)^{0{\cdot}03} \tag{5.1}$$

at fixed R_m', showing that the dependence of the amplification on the ratio of turbulent to field scale is small. Not too much significance is to be attached to the result (5.1) since the results of Sections 4(a) and (b) are produced from a rather small number of points, and addition of the results of another one or two computations might well change the index in relation (5.1) by as much as 100 per cent. The relevant conclusion is just that it is small.

FIG. 12. *Field lines for* $R_m = 80$ *at* $\tau = 20{\cdot}25$. $\langle B^2 \rangle = 0{\cdot}21$.

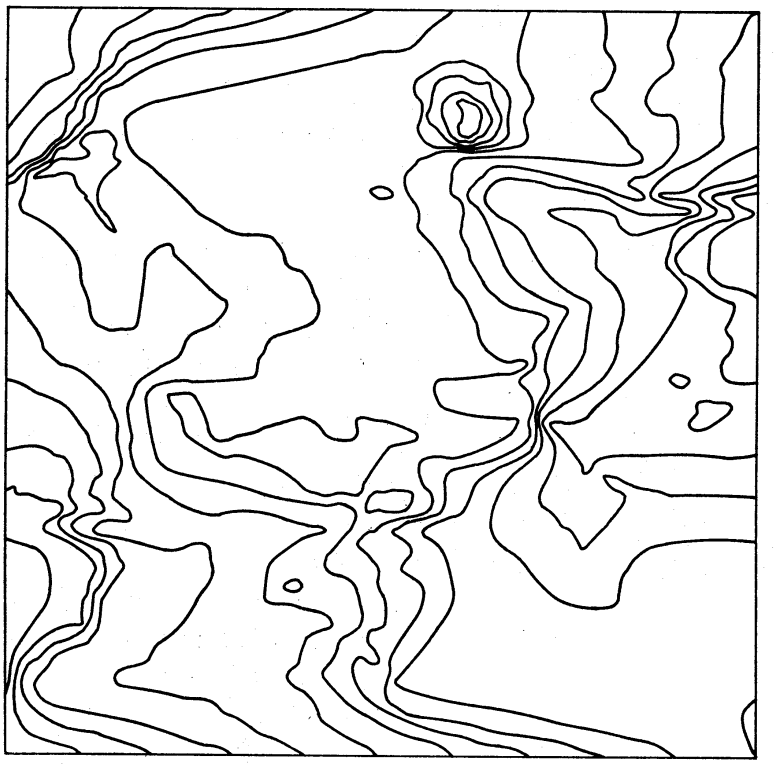

FIG. 13. *Field lines for* $R_m = 200$ *at* $\tau = 20{\cdot}25$. $\langle B^2 \rangle = 0{\cdot}44$.

6. ON THE EXPULSION OF FLUX FROM AN ISOLATED TURBULENT ZONE

In connection with the problem of the expulsion of flux from a convective zone computations were performed for cases for which, in the region $a/2 \geqslant |x| \geqslant a/4$, the velocities were zero, see Fig. 14. The boundary conditions on A were those used previously. Over the two columns of grid points next to the boundary of the ' dead zone ' the velocities were made to tend to zero.

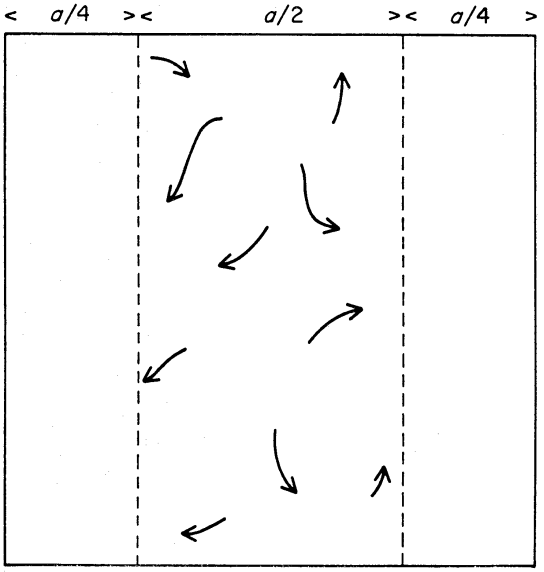

FIG. 14. *See text.*

This provided a ' dead zone ' into which it might have been possible for flux expelled from the turbulent zone to diffuse and be left undisturbed. Cases were run, for $R_m = 50$, $\Delta T' = 0{\cdot}90$, and $R_m = 50$ and 200, $\Delta T' = 0{\cdot}15$. (The velocity field as a function of time in the turbulent zone was the same as the velocity field in the corresponding region of the grid in the previous calculations.) Typical configurations of the field lines are shown in Figs 15 and 16. Fig. 16 can be compared with Fig. 13 which shows the same case at the same time for the previous computations with no dead zone. In addition, a case was run for a short time for which fluid in the region $a/2 \geq |y| \geq 5/14a$ also had zero velocity. The results were seen to be developing in a similar manner. In all these cases it is seen that flux is not expelled completely from the turbulent zone. There seems to be a tendency for regions to form from which most of the flux is expelled; these are separated by ' ropes ' of field lines which move in the fluid, and in these ropes the mean square field can reach high values. For typical configurations of the cases calculated above the mean value of B^2 in a region in the centre of the turbulent zone is listed in Table I. (Again the initial field was normalized so that $B_0^2 = 0{\cdot}0625$ in arbitrary units.) These figures can be compared with the mean values $\langle B^2 \rangle$ on the grid for the calculations with no dead zone at the same times. These values are also given in Table I. There $\langle B_t^2 \rangle$ is the mean value of B^2 in a region in the centre of the turbulent zone for the calculations with a dead zone. $\langle B_1^2 \rangle$ is the mean value of B^2 over the whole grid at the same time, and $\langle B_2^2 \rangle$ the value over the whole grid for the previous calculations with no dead zone.

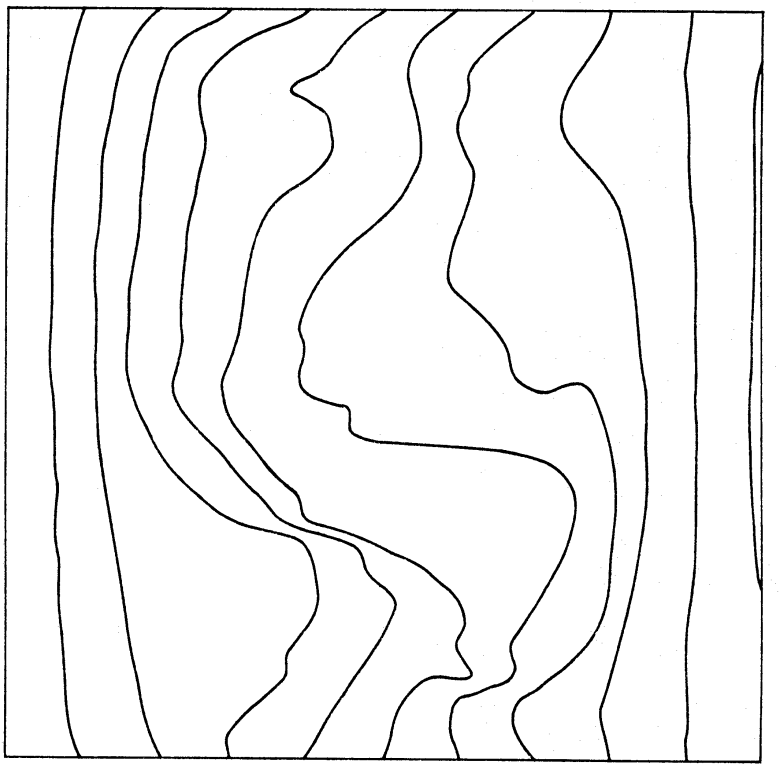

FIG. 15. *Field lines for* $R_m = 25$ *at* $\tau = 23{\cdot}1$ *for computations with a dead zone.*

FIG. 16. *Field lines for* $R_m = 200$ *at* $\tau = 20{\cdot}25$ *for computations with a dead zone.*

TABLE I

R_m	$\Delta T'$	τ	$\langle B_t^2 \rangle$	$\langle B_1^2 \rangle$	$\langle B_2^2 \rangle$
50	0·15	12·0	0·055	0·113	0·229
	0·15	23·1	0·084	0·102	0·180
	0·90	20·1	0·98	0·43	0·78
200	0·15	12·0	0·109	0·219	0·527
	0·15	20·25	0·099	0·155	0·529

It is seen that although, except in one case, the mean square field in the centre of the turbulent zone is less than that over the complete grid it is still, in three of the cases given, greater than the initial mean square field. In fact in order to avoid any edge effects the region over which $\langle B_t^2 \rangle$ was calculated was so small that the result $\langle B_t^2 \rangle = 0{\cdot}055$ is probably a consequence of this region falling between ' ropes ' of flux. The $R_m = 50$, $\Delta T' = 0{\cdot}90$ result is probably anomalous because the length scale of the turbulence is nearly as large as the size of the turbulent zone. No zones with the field completely expelled appeared in this case. Typically in the computations with $\Delta T' = 0{\cdot}15$, 40 to 60 per cent of the flux which originates between the planes $x = \pm a/4$ at the walls crosses $y = 0$ in the turbulent region, i.e. between $x = \pm a/4$. That is

$$\frac{A(x = a/4, y = 0, t) - A(x = -a/4, y = 0, t)}{A(x = a/4, y = a/2, t) - A(x = -a/4, y = a/2, t)} \sim 0{\cdot}4 \text{ to } 0{\cdot}6.$$

7. EXTENSION TO THREE DIMENSIONAL MOTIONS

The numerical results and order of magnitude arguments given above apply to two dimensional motions only. An extension to three dimensions would clearly be desirable. Parker (1963) gives a three-dimensional order of magnitude argument applicable to the problem described in Section 3, taking $T_{\max}$, relation (3.5), to be essentially λ/v_t, and gets $\langle\langle B^2 \rangle\rangle_t \propto R_m^{1/2}$, compared with $\langle\langle B^2 \rangle\rangle_t \propto R_m$ for the same basic argument applied to motions in two dimensions. The argument given in Section 3 is not easily extendable since there is no estimate analogous to relation (3.2) available for three-dimensional cells. If, however, this estimate

$$T_{\max} \alpha \frac{L}{U} R_{mc}{}^{\alpha}$$

is retained then conservation of flux gives $l \sim a/\xi^2$. and so relation (3.3) becomes

$$T_{\max} \sim \frac{L^2}{\xi^4 \eta} \sim \frac{R_m{}^{2\alpha/(1+\alpha)}}{\Delta T^{(1-\alpha)/(1+\alpha)}} \left(\frac{L}{v_t}\right)^{2/(1+\alpha)}, \tag{7.1}$$

implying

$$\xi^2 \sim \frac{\langle\langle B^2 \rangle\rangle_t}{B_0{}^2} \sim (R_m \Delta\tau)^{(1-\alpha)/2(1+\alpha)} \tag{7.2}$$

which has again half the growth rate as a function of R_m of the two-dimensional case for the same value of α.

For the maximum value of the squared field, $\langle B_{\max}{}^2 \rangle_t$, it can be argued that the amplification factor in three dimensions is the square of that in two, since the field can now be concentrated in two dimensions. This argument was given by Weiss for three-dimensional regular cells, but in applying it to turbulent motions it must be

realized that neighbouring turbulent eddies cannot be coordinated, as cells can be, to simultaneously compress the field at their common boundary. However such coordination will occur randomly, and so this may be a valid estimate for $\langle B_{\max}^2 \rangle_t$ over a large enough volume of fluid. The result of Section 4(d) would then imply $\langle B_{\max}^2 \rangle_t \gtrsim R_m^{2.5}$ for three-dimensional motions.

8. DISCUSSION AND CONCLUSION

The results described above give the degree of amplification of the mean square field expected to be caused by an isotropic, two-dimensional, statistically steady turbulent velocity field acting on a maintained seed field. Although the turbulent velocity field considered is rather artificial in form, it seems plausible that the nature of the results should be applicable to more general turbulent motions. The results described in Section 4 give support to the view that, if the Lorentz forces acting on the fluid are ignored, the growth of a field maintained by an external e.m.f. will ultimately be halted by resistive effects. The extension of these results to three-dimensional motions such as occur in nature is rather speculative. However there is no clear reason why the amplification of the field should not be halted eventually by resistive effects in three dimensions also. But to describe motions with Reynolds numbers of the order of magnitude of those occurring astrophysically considerable extrapolation of the above results is needed. Given the validity of this, the amplification factors may be very large indeed, and often sufficient to amplify the energy density of a large scale maintained seed field to equipartition with the kinetic energy density of the turbulence. This is as much as could be done by turbulent motions even if it were true that, by ignoring the magnetic forces acting on the fluid, fields could be amplified indefinitely. However this investigation throws no light on the problem of whether the field energy would reach equipartition with the kinetic energy of the entire spectrum of the turbulence or with that of the large wavenumber component (e.g. Batchelor 1950).

A place where turbulent gas motions and a magnetic field seem to be interacting is the disc of the Galaxy. A state with approximate equipartition of the small-scale field energy and the gas kinetic energy may have been reached. Reynolds numbers of the turbulent motions in the disc are very large (a typical velocity is 10^6 cm s^{-1}, a length scale is 10^{20} cm and $\eta \sim 10^{10}$ c.g.s.; so $R_m \sim 10^{16}$), and so any of the estimates given in Section 7 predict a very large amplification of a large-scale field, which would be adequate to bring any but a very small large-scale field up to equipartition values. In a cloudy region of the Perseus arm measurements of the Zeeman splitting of the 21-cm line suggest the presence of fields of $\sim 2.10^{-5}$ gauss. Local values for the magnetic energy above the mean equipartition value are of course to be expected in a turbulent regime. Fields of such strength possibly present difficulties in the theory of star formation, but a possible solution to the problem is that, when a gas cloud becomes denser and more massive than average (e.g. by collisions), and then gains by chance a kinetic energy greater than the equipartition value, it is able to control the magnetic field threading it, and to bend this field so much that it disconnects from the local large-scale field. Fig. 17 shows schematically the development of this process.

The field inside the cloud, having been disconnected from the outside field, can decay rapidly, this process perhaps being aided by further reduction of the field scale by turbulent motions inside the gas cloud. Thus the field becomes less able to

prevent contraction. Alternatively, if a blob of gas did manage to start contracting, it would be expected to amplify the field inside it.

Another place where it has been suggested that the interaction of a magnetic field and turbulence may be important is in the convection zones of stars undergoing pre-main sequence evolution down the Hayashi track. A strong enough field may or may not be able to affect the nature of the convection. This problem was discussed in Moss & Tayler (1969). If the field is weaker, it may not be able to affect the convection in the Hayashi phase, but if the field were able to survive this phase it possibly could be of importance in the main sequence or later stages of evolution. It

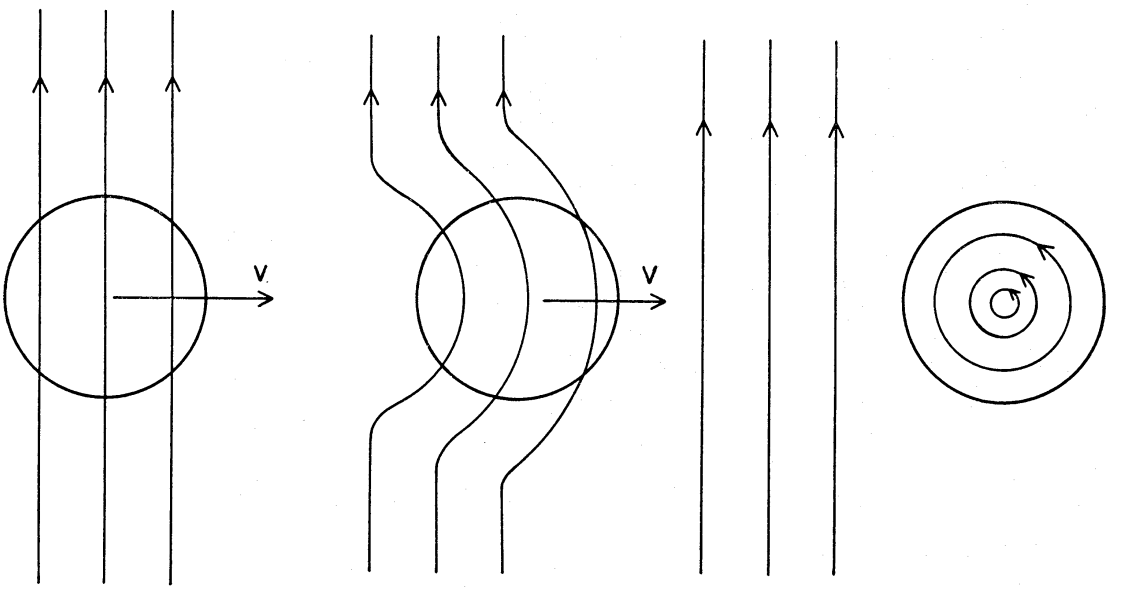

FIG. 17. *Schematic detachment of gas cloud from large-scale magnetic field.*

is not clear (e.g. Mestel (1967)) whether or not a large-scale magnetic field threading a star could survive the Hayashi phase. Although the turbulence in such a case will not be isotropic, the computations described in Section 6 suggest that the magnetic field may not be expelled completely from the turbulent zone, but instead be concentrated into ropes which are convected around without having any significant effect on the structure of the region as a whole. When the convection dies away the field will still be there, and may later be able to influence processes in the remaining zone. However these results were obtained at rather low Reynolds numbers.

The subphotospheric convection zone in the Sun is also a place where magnetic fields may be interacting with convection. In sunspots strong fields are observed, coupled, apparently, with local inhibition of convection. It might be possible to associate the sunspot fields with ropes of flux as produced by (non-isotropic) turbulent motions in the deep convection zone but it seems likely, in view of the evidence for large-scale cellular networks in the solar surface (e.g. Simon & Weiss 1969), that these are associated with more regular motions. However it is possible that a turbulent process could be important for the field on a smaller scale. It is worth noting that in the photosphere, where an estimate of the large-scale field is 1 gauss, and where the Reynolds number is about 10^6 (e.g. Weiss 1964) the discussion of Section 7 only predicts amplification of the mean field by about an order of magnitude, whereas the maximum field might be increased to well above equipartition values ($\sim 6.10^2$ gauss).

This investigation has not been directly applicable to a true dynamo process in which there is no externally maintained seed field. The latter problem has aroused much interest and discussion, e.g. Biermann & Schluter (1951), Saffman (1964), Cowling (1965) and Vainshtein (1969). There is dispute as to whether an initial weak magnetic field can be amplified to, and maintained at, equipartition with the velocity field, or at least amplified so that the r.m.s. field has an oscillatory steady state around a value greater than that of the initial field. The alternative is that the decrease in length scale of the magnetic field caused by the turbulent motions eventually enhances the resistive decay so much that the field dies away. However Zeldovich (1956) has shown that a two-dimensional isotropic turbulent dynamo cannot exist, and computations by Moss (1969) at low Reynolds numbers support his results. If the result that a maintained seed field cannot be amplified indefinitely by two-dimensional motions is extendable to motions in three dimensions, (and the discussion of Section 7 of this chapter suggests that the amplification factor for the r.m.s. field as a function of Reynolds number may be smaller for three-dimensional than two-dimensional motions) then it is perhaps unlikely that a turbulent dynamo maintained by three-dimensional motions can exist. Various theoretical investigations, e.g. Cocke (1968), Vainshtein (1969), support this view.

Although, as has been emphasized, the computations were all carried out for comparatively low magnetic Reynolds numbers, they do confirm the order of magnitude arguments which are formally independent of the size of the Reynolds number. If the extrapolation to the higher Reynolds numbers is valid, it seems that turbulent motions occurring astrophysically will often be able to amplify a large-scale field to equipartition with the energy of some part of the spectrum of fluid motions. However the scale of the field will be correspondingly reduced. By comparing the results (4.1), (4.2), (4.3) with the results of Weiss (1966) and Moss (1969) for regular cellular motions it seems that the turbulent velocity field produces a larger amplification, as a function of Reynolds number, for both the mean and maximum fields than more regular motions. The turbulent motions considered produce large oscillations of the mean square field, even when a statistically steady state seems to have been reached.

ACKNOWLEDGMENTS

This work was begun whilst at the Astronomy Centre, University of Sussex, and finished at the Department of Astronomy, Columbia University, New York. I thank Professor R. J. Tayler for his advice. I am grateful for the award of an S.R.C. Research Studentship, and an E.S.R.O./N.A.S.A. Research Fellowship during the tenure of which this work was done.

Department of Astronomy, Columbia University, New York, N.Y. 10027.

Received in original form 1969 *October* 13.

REFERENCES

Batchelor, G. K., 1950, *Proc. R. Soc. Lond. A*, **201**, 405.
Biermann, L. & Schluter, A., 1951. *Phys. Rev.*, **82**, 863.
Cocke, W. J., 1968. Preprint.
Cowling, T. G., 1965. In '*Stellar and Solar Magnetic Fields*', I.A.U. Symposium No. 22, Amsterdam.

Mestel, L., 1967. In '*Astrofisica del plasma*'. Enrico Fermi School XXXIX. Academic Press.
Moss, D. L., 1969. Doctoral Thesis, University of Sussex.
Moss, D. L. & Tayler, R. J., 1969. *Mon. Not. R. astr. Soc.*, **145,** 217.
Parker, E. N., 1963. *Astrophys. J.*, **138,** 226.
Saffman, P. G., 1963. *Jl Fluid Mech.*, **16,** 545.
Saffman, P. G., 1964. *Jl Fluid Mech.*, **18,** 449.
Simon, G. W. & Weiss, N. O., 1969. *Z. Astrophys.*, **69,** 435.
Vainshtein, S. I., 1969. *Sov. Astr.*, **12,** 589.
Weiss, N. O., 1964. *Mon. Not. R. astr. Soc.*, **128,** 225.
Weiss, N. O., 1966. *Proc. R. Soc. Lond. A*, **293,** 310.
Zeldovich, Y. B., 1956. *J. exp. theor. Phys.*, **31,** 460.